Dynamics of a Space Robot Subjected to an Impact

Simone Manfredi

Università degli Studi di Trento

Table of Contents

1.0 Introduction:

Introduction

1.0 Introduction:

- Thesis' aim: satellite docking, stabilization and inertia retrieval.
- Docking → *impact*.
- Manipulator → robotic arm:
  - Rigid bodies: *links*
  - Relative motion: *joints*
  - Actuation: *motors*
- Vehicle-Manipulator System: VMS.

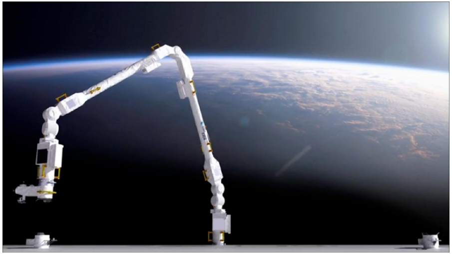

Figure 1: ESA's space manipulator [1].

Table of Contents

2.0 Overview:

Historical Background

2.0 Overview:

- First space manipulator: Space Remote Manipulator System (SRMS), 11/1981 - 07/2011.
- First space mission: MIR, 1986 - 2001.
- Japanese arm: 2008.
- Canadarm2 (or SSRMS) and MSS: 04/2001
- ESA's manipulator, ERA: 07/2021

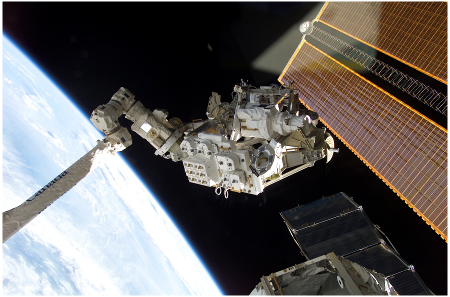

Figure 2: Canadarm2 attached to the Mobile Base System [2].

Main Characteristics

2.0 Overview:

- Lack of fixed base:
  - Free-flying system;
  - Free-floating system.
- Typical capture sequance:
  1. observation and planning phase;
  2. final approach phase;
  3. impact and grasping/capture phase;
  4. post-capture stabilization phase.
- To avoid impact: zero relative velocity.

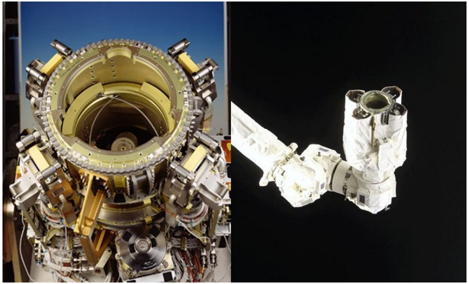

Figure 3: Latching End Effector (LEE) [2].

Main Characteristics
2.0 Overview:

- Two 2-links arms attached to a ”shoulder”.
- Usually redundant kinematics.
- Number of degrees of freedom:
  $n = 3(m-1) - 2c_1 - c_2$

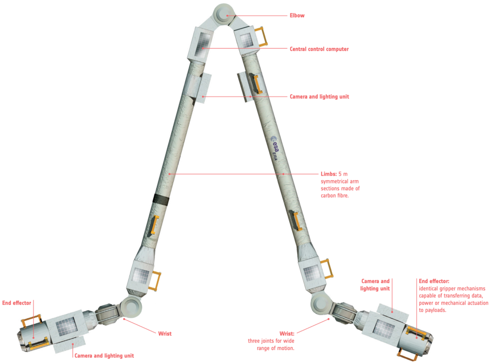

Figure 4: ERA specifications [3].

Table of Contents

3.0 Kinematics:

Fundamentals

3.0 Kinematics:

- Roto-Translation Matrix:

$$ {}^{f}\begin{bmatrix} O_fP_x \\ O_fP_y \\ O_fP_z \\ 1 \end{bmatrix} = \begin{bmatrix} {}^{f}_{m}R & {}^{f}\begin{bmatrix} O_fO_mx \\ O_fO_my \\ O_fO_mz \end{bmatrix} \\ 0 & 1 \end{bmatrix} {}^{m}\begin{bmatrix} O_mP_x \\ O_mP_y \\ O_mP_z \\ 1 \end{bmatrix} = {}^{f}_{m}M \, {}^{m}\begin{bmatrix} O_mP_x \\ O_mP_y \\ O_mP_z \\ 1 \end{bmatrix} \tag{1} $$

- Veolocity Matrix: ${}^{f}W = {}^{f}_{m}\dot{M}\, {}^{m}_{f}M$

$$ W = \begin{bmatrix} 0 & -\omega_z & \omega_y & v_x \\ \omega_z & 0 & -\omega_x & v_y \\ -\omega_y & \omega_x & 0 & v_z \\ 0 & 0 & 0 & 0 \end{bmatrix} \tag{2} $$

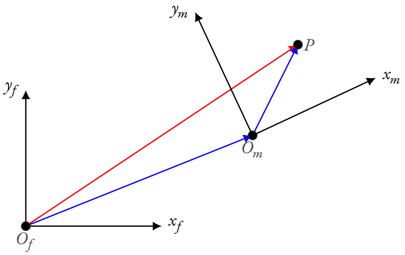

Figure 5: Definition of a point in a rotated and translated frame with respect to the fixed one.

Danavit-Hartenberg Method

3.0 Kinematics:

- Used to define reference frames.
- Ordered procedure:
    1. z_i axis: axis of the revolute joint that connects the link to the following.
    2. x_i axis: line of minimum distance between z_{i-1} and z_i, oriented from z_{i-1} to z_i.
    3. y_i axis: obtained by the vectorial product of the other two axes.

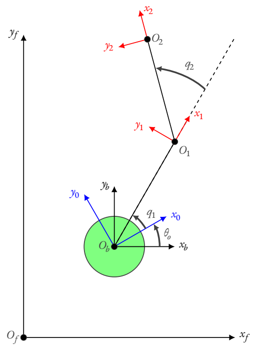

Figure 6: The Danavit-Hartenberg rule has been used to place the local joints' frame (in red) in a planar RR manipulator.

Planar VMS

3.0 Kinematics:

- VMS' coordinates: $p = \{x_b, y_b, \theta_b, q_1, q_2\}$
- Satellite coordinates: $\psi = \{x_O, y_O, \theta_O\}$

$$
\begin{gathered}
{}^{f}_{b}M = \begin{bmatrix} 1 & 0 & 0 & x_b \\ 0 & 1 & 0 & y_b \\ 0 & 0 & 1 & 0 \\ 0 & 0 & 0 & 1 \end{bmatrix} \quad {}^{b}_{0}M = \begin{bmatrix} \cos\theta_0 & -\sin\theta_0 & 0 & 0 \\ \sin\theta_0 & \cos\theta_0 & 0 & 0 \\ 0 & 0 & 1 & 0 \\ 0 & 0 & 0 & 1 \end{bmatrix} \\
{}^{0}_{1}M = \begin{bmatrix} \cos q_1 & -\sin q_1 & 0 & l_1\cos q_1 \\ \sin q_1 & \cos q_1 & 0 & l_1\sin q_1 \\ 0 & 0 & 1 & 0 \\ 0 & 0 & 0 & 1 \end{bmatrix} \quad {}^{1}_{2}M = \begin{bmatrix} \cos q_2 & -\sin q_2 & 0 & l_2\cos q_2 \\ \sin q_2 & \cos q_2 & 0 & l_2\sin q_2 \\ 0 & 0 & 1 & 0 \\ 0 & 0 & 0 & 1 \end{bmatrix}
\end{gathered} \tag{3}
$$

Planar VMS

3.0 Kinematics:

$$p_{EE} = {}^{0}_{2}MO_3 = \begin{bmatrix} l_1\cos(\theta_0 + q_1) + l_2\cos(\theta_0 + q_1 + q_2) + x_b \\ l_1\sin(\theta_0 + q_1) + l_2\sin(\theta_0 + q_1 + q_2) + y_b \\ 0 \\ 1 \end{bmatrix} \tag{4}$$

with $O_3 = \{0, 0, 0, 1\}$.

$${}^{f}W_{f1_{1:3,1:3}} = \begin{bmatrix} 0 & -\dot{\theta}_0 - \dot{q}_1 & 0 \\ \dot{\theta}_0 + \dot{q}_1 & 0 & 0 \\ 0 & 0 & 0 \end{bmatrix} \quad {}^{f}W_{f2_{1:3,1:3}} = \begin{bmatrix} 0 & -\dot{\theta}_0 - \dot{q}_1 - \dot{q}_2 & 0 \\ \dot{\theta}_0 + \dot{q}_1 + \dot{q}_2 & 0 & 0 \\ 0 & 0 & 0 \end{bmatrix} \tag{5}$$

$${}^{f}L_{f1_{1:3,1:3}} = \begin{bmatrix} 0 & -1 & 0 \\ 1 & 0 & 0 \\ 0 & 0 & 0 \end{bmatrix} \quad {}^{f}L_{f2_{1:3,1:3}} = \begin{bmatrix} 0 & -1 & 0 \\ 1 & 0 & 0 \\ 0 & 0 & 0 \end{bmatrix} \tag{6}$$

Satellite Kinematics

3.0 Kinematics:

$$
{}^{f}_{O_0}M = \begin{bmatrix} 1 & 0 & 0 & x_O \\ 0 & 1 & 0 & y_O \\ 0 & 0 & 1 & 0 \\ 0 & 0 & 0 & 1 \end{bmatrix} \quad {}^{O_0}_{O_1}M = \begin{bmatrix} \cos\theta_O & -\sin\theta_O & 0 & 0 \\ \sin\theta_O & \cos\theta_O & 0 & 0 \\ 0 & 0 & 1 & 0 \\ 0 & 0 & 0 & 1 \end{bmatrix}
$$

$$
{}^{O_1}_{O_2}M = \begin{bmatrix} \cos\gamma & -\sin\gamma & 0 & r\cos\gamma \\ \sin\gamma & \cos\gamma & 0 & r\sin\gamma \\ 0 & 0 & 1 & 0 \\ 0 & 0 & 0 & 1 \end{bmatrix} \tag{7}
$$

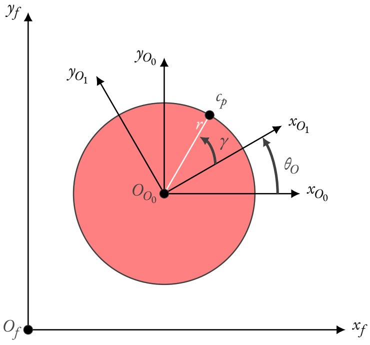

Figure 7: Tumbling object disk approximation.

Table of Contents
4.0 Dynamics:

Fundamentals

4.0 Dynamics:

- Direct Dynamics.
- Inverse Dynamics.
- Given a *wrench* w at the EE:
  - Power at the joints: $P_\tau = \tau_w^T \dot{q}$
  - Power at the EE: $P_e = w^T v$
  - Conservation of energy:

$$P_\tau = P_e \quad \Longrightarrow \quad \tau_w^T \dot{q} = w^T v = w^T J \dot{q} \quad \forall \dot{q} \Longrightarrow \quad \tau_w^T = w^T J \quad \Longrightarrow \quad \tau_w = J^T w$$

- Equation of motion: $M(q)\ddot{q} + C(q,\dot{q}) = u + J^T(q)w$

VMS

4.0 Dynamics:

- Homogeneous Matrix Approach [4, 5].
- Lagrangian formulation:

$$\mathcal{L}(q, \dot{q}) = \sum_{i=1}^{N} T_i - U_i, \qquad \frac{d}{dt}\frac{\partial \mathcal{L}}{\partial \dot{q}_i} - \frac{\partial \mathcal{L}}{\partial q_i} = f_i \tag{8}$$

- Action Matrix:

$$^{i}\phi_k = \begin{bmatrix} 0 & -c_z & c_y & f_x \\ c_z & 0 & -c_x & f_y \\ -c_y & c_x & 0 & f_z \\ -f_x & -f_y & -f_z & 0 \end{bmatrix} \tag{9}$$

- Non-Lagrangian components:

$$f_{q_i} = \left(\sum_{j=1}^{N} {}^{f}\phi_j \right) \otimes {}^{f}L_{q_i} \tag{10}$$

VMS

4.0 Dynamics:

- Non-Lagrangian components:

$$
\begin{aligned}
f_1 &= \left({}^f\phi_b + {}^f\phi_1 + {}^f\phi_2\right) \otimes {}^f L_{fb_x} = F_x \cos\theta_0 - F_y \sin\theta_0 \\
f_2 &= \left({}^f\phi_b + {}^f\phi_1 + {}^f\phi_2\right) \otimes {}^f L_{fb_y} = F_x \sin\theta_0 + F_y \cos\theta_0 \\
f_3 &= \left({}^f\phi_b + {}^f\phi_1 + {}^f\phi_2\right) \otimes {}^f L_{f0} = \tau_0 \\
f_4 &= \left({}^f\phi_b + {}^f\phi_1\right) \otimes {}^f L_{01} = \tau_1 \\
f_5 &= {}^f\phi_b \otimes {}^f L_{12} = \tau_2
\end{aligned}
\tag{11}
$$

- Kinetic Energy

$$
T_j = \frac{1}{2}\,\mathrm{Tr}\left({}^f W_{fj}\, {}^f J_j\, {}^f W_{fj}^T\right) \tag{12}
$$

Table 1: Moments of inertia of the planar VMS' bodies, with respect to their centre of mass (in the centre of the base and the arms), with $i = \{1, 2\}$.

Body	Tensor of Pseudo Inertia
Base	$\begin{bmatrix} \frac{1}{4}m_b r^2 & 0 & 0 \\ 0 & \frac{1}{4}m_b r^2 & 0 \\ 0 & 0 & 0 \end{bmatrix}$
Arms	$\begin{bmatrix} \frac{1}{3}m_i l_i^2 & 0 & 0 \\ 0 & 0 & 0 \\ 0 & 0 & 0 \end{bmatrix}$

Satellite

4.0 Dynamics:

- Same procedure or, alternatively:

$$T_O = v_O m_O v_O^T + \frac{1}{2} I_{O_z} \theta_O^2 \tag{13}$$

- Mass matrix:

$$M_O = \begin{bmatrix} m_O & 0 & 0 \\ 0 & m_O & 0 \\ 0 & 0 & \frac{m_O r^2}{2} \end{bmatrix} \tag{14}$$

Table of Contents
5.0 Impact Analysis:

Conservation of Momentum

5.0 Impact Analysis:

- Four assumptions [6]:
  - Only the generalized velocities change during the impat, no displacement.
  - At the contact point between the end-effector and the target there are no forces but moments only.
  - We know the satellite's mass and initial velocities.
  - Plastic impact.
- Equations of motion:

$$\begin{cases} M\ddot{p} + C = u + J^T f_I \\ M_O\ddot{\psi} + C_O = -J_O^T f_I \end{cases} \tag{15}$$

and

$$\int_0^{\pi} M\ddot{p}\,dt + \int_0^{\pi} C\,dt = -\int_0^{\pi} J^T (J_O^+)^T M_O \ddot{\psi}_O\,dt + \int_0^{\pi} (u - J^T (J_O^+)^T C_O)\,dt \tag{16}$$

- Conservation of momentum equation:

$$M(\dot{p}_f - \dot{p}_i) + J^T (J_O^+)^T M_O(\dot{\psi}_f - \dot{\psi}_i) = 0 \tag{17}$$

- For one degree of freedom:

$$m_1(v_{f,1} - v_{i,1}) + m_2(v_{f,2} - v_{i,2}) = 0 \tag{18}$$

- For plastic impacts:

$$J\dot{p}_f = J_O\dot{\psi}_f \quad \Longrightarrow \quad \dot{\psi}_f = J_O^+ J\dot{p}_f \tag{19}$$

- Substituting (19) in (17):

$$\dot{p}_f = G^{-1}H \tag{20}$$

where:

$$\begin{aligned} G &= M + J^T (J_O^+)^T M_O J_O^+ J \\ H &= M\dot{p}_i + J^T (J_O^+)^T M_O \dot{\psi}_i \end{aligned} \tag{21}$$

- New equation after impact:

$$\dot{\psi}_f = J_O^+ J \dot{p}_f \quad \Longrightarrow \quad \ddot{\psi} = J_O^+ J \ddot{p} + \frac{\partial J_O^+}{\partial t} J \dot{p} + J_O^+ \frac{\partial J}{\partial t} \dot{p} \tag{22}$$

$$\begin{cases} M\ddot{p} + C = u + J^T f_I \\ M_O \ddot{\psi} + C_O = -J_O^T f_I \end{cases}$$

$$M' \ddot{p} + C' = u \tag{23}$$

where:

$$\begin{aligned} M' &= M + J^T (J_O^T)^+ M_O J_O^+ J \\ C' &= C + J^T (J_O^T)^+ M_O \frac{\partial J_O^+}{\partial t} J \dot{p} + J^T (J_O^T)^+ M_O J^+ \frac{\partial J}{\partial t} \dot{p} + J^T (J_O^T)^+ C_O \end{aligned} \tag{24}$$

Table 2: VMS parameters.

l_1	l_2	m_b	m_1	m_2	m_O	r	γ
5.59 m	5.59 m	419 725 kg	300 kg	300 kg	3000 kg	0.12 m	0.5 rad

Table 3: Simulation's initial positions.

x_b	y_b	θ_0	q_1	q_2	x_O	y_O	θ_O
4 m	2 m	$\pi/2$ rad	0 rad	$\pi/2$ rad	−1.71 m	7.59 m	5.78 rad

Table 4: Simulation's initial velocities.

	Simulation 1	Simulation 2
$\dot{\theta}_0$	$0\,\mathrm{rad\,s^{-1}}$	$0\,\mathrm{rad\,s^{-1}}$
$\dot{x}_b$	$0\,\mathrm{m\,s^{-1}}$	$0\,\mathrm{m\,s^{-1}}$
$\dot{y}_b$	$0\,\mathrm{m\,s^{-1}}$	$0\,\mathrm{m\,s^{-1}}$
$\dot{q}_1$	$0\,\mathrm{rad\,s^{-1}}$	$0\,\mathrm{rad\,s^{-1}}$
$\dot{q}_2$	$0\,\mathrm{rad\,s^{-1}}$	$0\,\mathrm{rad\,s^{-1}}$
$\dot{x}_O$	$1\,\mathrm{m\,s^{-1}}$	$0\,\mathrm{m\,s^{-1}}$
$\dot{y}_O$	$0\,\mathrm{m\,s^{-1}}$	$-1\,\mathrm{m\,s^{-1}}$
$\dot{\theta}_O$	$0.01\,\mathrm{rad\,s^{-1}}$	$0.01\,\mathrm{rad\,s^{-1}}$

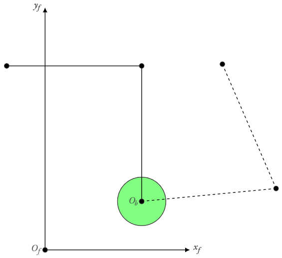

(a) *Simulation 1.*

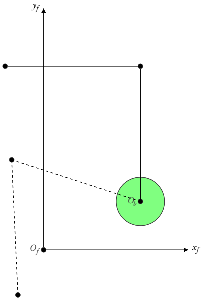

(b) *Simulation 2.*

Figure 8: Initial and final (dashed) position of the VMS after the impact for the two different simulations, ten seconds long.

Rigid Bodies

5.0 Impact Analysis:

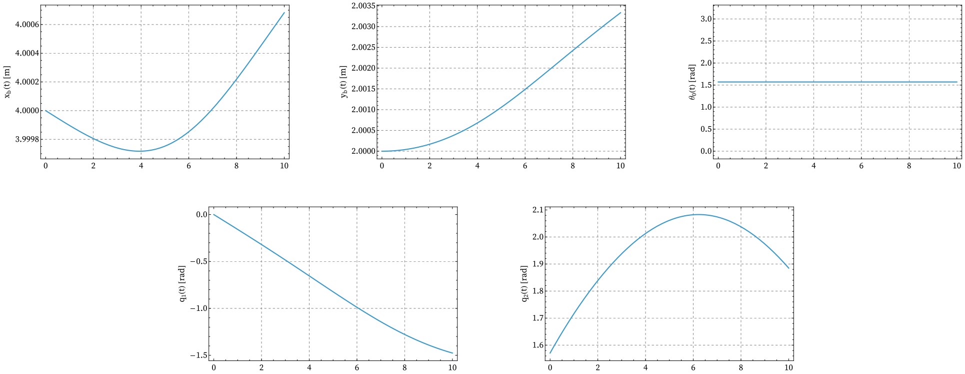

Figure 9: VMS generalized coordinates' displacement after the catching of the payload when no control is performed, Simulation 1.

Rigid Bodies

5.0 Impact Analysis:

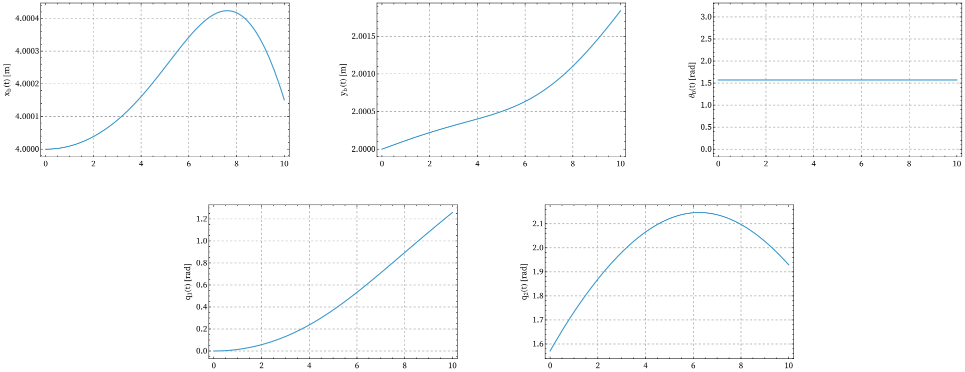

Figure 10: VMS generalized coordinates' displacement after the catching of the payload when no control is performed, Simulation 2.

Rigid Bodies

5.0 Impact Analysis:

- Controlled motion:

$$\begin{bmatrix} M'_{tt} & M'_{tr} \\ M'_{rt} & M'_{rr} \end{bmatrix} \begin{bmatrix} \ddot{p}_t \\ \ddot{p}_r \end{bmatrix} + \begin{bmatrix} C'_t \\ C'_r \end{bmatrix} = \begin{bmatrix} 0 \\ u \end{bmatrix} \tag{25}$$

- Translational coordinates as a function of rotational ones:

$$\ddot{p}_t = -{M'}^{-1}_{tt} (M'_{tr} \ddot{p}_r + C'_t) \tag{26}$$

- Final equation:

$$\ddot{p}_r \tilde{M} + \tilde{C} = u \tag{27}$$

- Feedback linearization:

$$u = \hat{M}[\ddot{q}_d + K_d(\dot{q}_d - \dot{q}) + K_p(q_d - q)] + \hat{C} \tag{28}$$

- If $\hat{M} \approx \tilde{M}$ and $\hat{C} \approx \tilde{C}$:

$$\ddot{e} + K_d\dot{e} + K_p e = 0 \tag{29}$$

  - decoupled;
  - linear;
  - $\omega_n = \sqrt{K_{p_i}}$ and $\xi = \frac{K_{d_i}}{2\sqrt{K_{p_i}}}$.

- Critically damped when

$$\xi = 1 \quad \Longrightarrow \quad K_d = 2\sqrt{K_p} \tag{30}$$

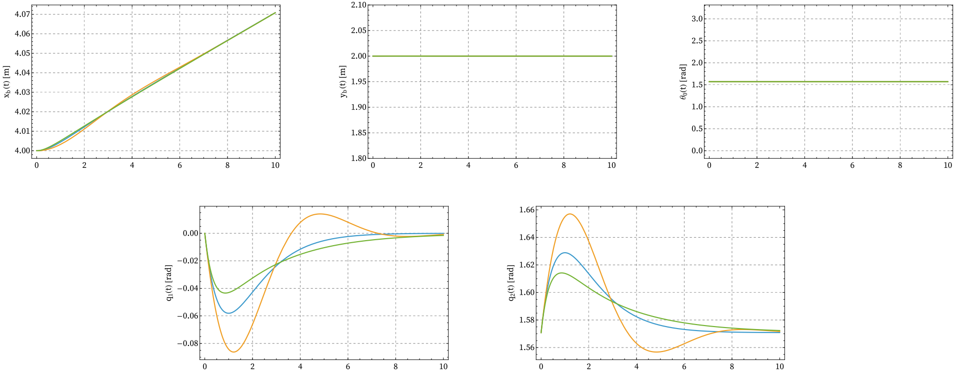

Figure 11: VMS generalized coordinates' displacement after the catching of the payload when control is performed, Simulation 1. In yellow, an underdamped behaviour ($\xi = 0.5$), in blue a critically damped behaviour ($\xi = 1$), in green an overdamped behaviour ($\xi = 1.5$).

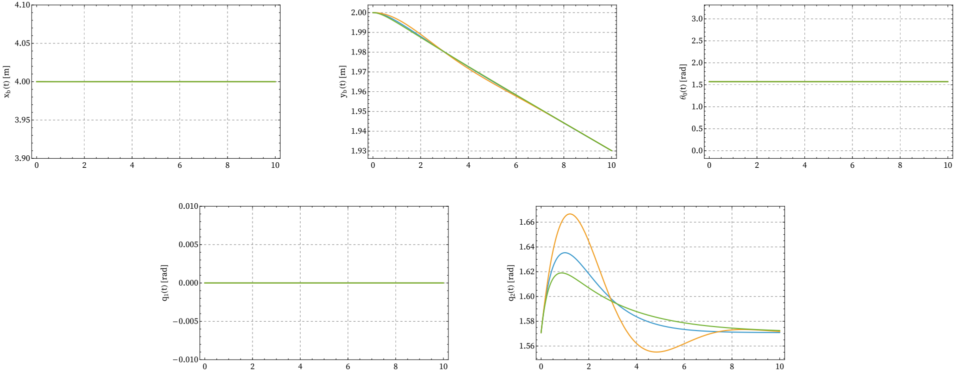

Figure 12: VMS generalized coordinates' displacement after the catching of the payload when control is performed, Simulation 2. In yellow, an underdamped behaviour ($\xi = 0.5$), in blue a critically damped behaviour ($\xi = 1$), in green an overdamped behaviour ($\xi = 1.5$).

- Arms modeled ad Euler-Bernoulli Beams:

$$\begin{aligned} w(x,t) &= \sum_{n=1}^{\infty} W_n(x) Q_n(t) \\ Q(t) &= A\cos\omega t + B\sin\omega t \\ W(x) &= c_1\cos(\beta x) + c_2\sin\beta x + c_3\cosh\beta x + c_4\sinh\beta x \end{aligned} \tag{31}$$

- Elasticity Matrix [7]:

$${}^{i}_{i+1}E = \begin{bmatrix} 1 & 0 & 0 & 0 \\ 0 & 1 & 0 & W_i(x)Q_i(t) \\ 0 & 0 & 1 & 0 \end{bmatrix} \tag{32}$$

- The number of coordinates increases: $p = \{x_b, y_b, \theta_b, q_1, q_2, Q_1, Q_2\}$.

Elastic Bodies

5.0 Impact Analysis:

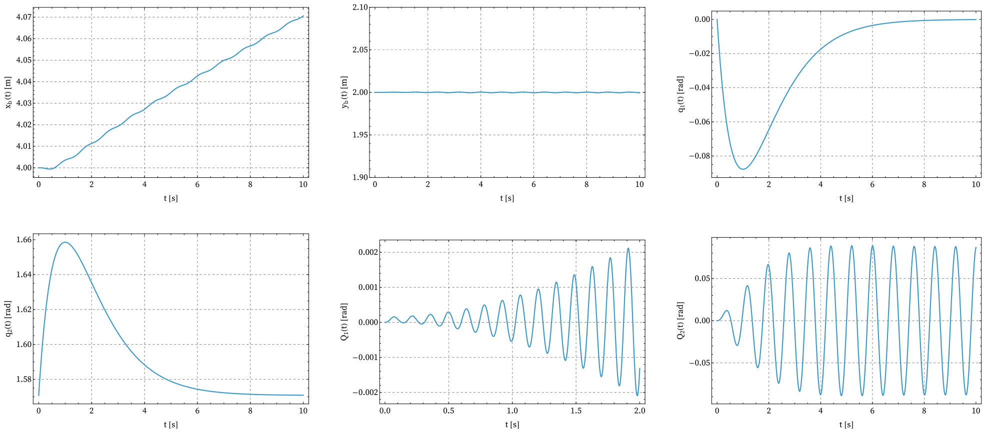

Figure 13: VMS generalized coordinates' displacement after the catching of the payload when control is performed, Simulation 1. Arms modeled as Euler-Bernoulli beams.

Elastic Bodies

5.0 Impact Analysis:

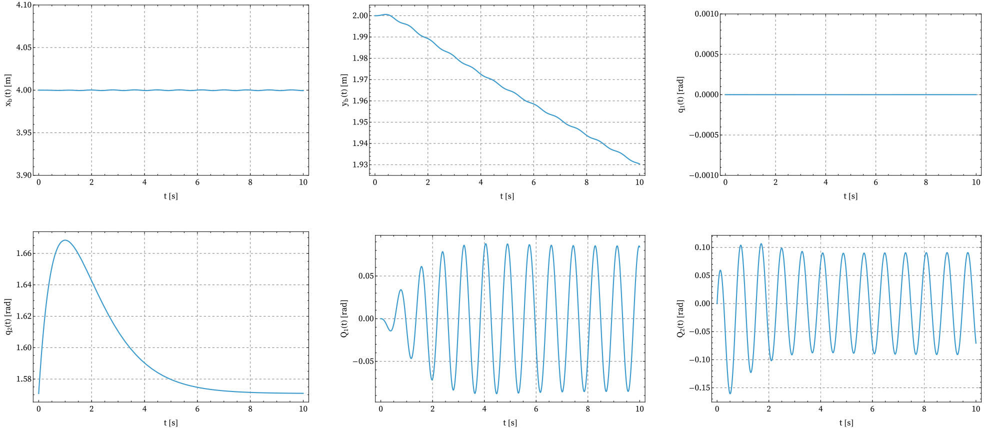

Figure 14: VMS generalized coordinates' displacement after the catching of the payload when control is performed, Simulation 2. Arms modeled as Euler-Bernoulli beams.

Table of Contents
6.0 Mass and Velocity Retrieval:

Linearization

6.0 Mass and Velocity Retrieval:

- Approximations:
  - No spacecraft translation;
  - No spacecraft rotation;
  - Linearization around equilibrium position.
- First-order Taylor expansion:

$$D(\mathrm{x}) = D(q_1, q_2, \dot{q}_1, \dot{q}_2, \ddot{q}_1, \ddot{q}_2) = M'(q_1, q_2)\begin{bmatrix}\ddot{q}_1 \\ \ddot{q}_2\end{bmatrix} + C'(q_1, q_2, \dot{q}_1, \dot{q}_2) \tag{33}$$

$$D(\mathrm{x}) \approx D(\bar{\mathrm{x}}) + (\mathrm{x} - \bar{\mathrm{x}})^T \nabla T(\mathrm{x}) \tag{34}$$

- New linearized dynamics:

$$M_{lin}\ddot{q} + C_{lin}\dot{q} + K_{lin}q - \delta = 0 \tag{35}$$

- Displacement of one arm negligible for the displacement of the other one (true when $\hat{M} = M'$).
- New equations:

$$\begin{aligned} \ddot{q}_1 + \frac{\hat{m}_1}{\tilde{m}_1} k_d \dot{e}_1 + \frac{\hat{m}_1}{\tilde{m}_1} k_p e_1 &= 0 \\ \ddot{q}_2 + \frac{\hat{m}_2}{\tilde{m}_2} k_d \dot{e}_2 + \frac{\hat{m}_2}{\tilde{m}_2} k_p e_2 &= 0 \end{aligned} \tag{36}$$

- Damping coefficient:

$$\xi' = \frac{\hat{m} k_v}{2\omega_n \tilde{m}} = \frac{\hat{m} 2\sqrt{k_p}}{2\sqrt{\frac{\hat{m}}{\tilde{m}} k_p \tilde{m}}} = \sqrt{\frac{\hat{m}}{\tilde{m}}} \tag{37}$$

Joints' Decoupling

6.0 Mass and Velocity Retrieval:

- Position Roots: find overshoot, find parametrix solution of equation and solve: $q(t^*, \tilde{m}) = q^*$.
- Mass Fit: minimize error with non-linear regression, parameter is the mass. We can add noise ($w(t) \sim \mathcal{N}(0, 0.005)$):

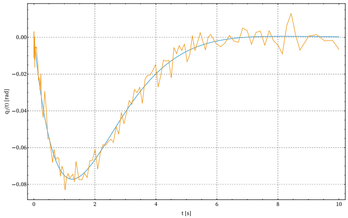

Figure 15: Noisy data to simulate a real scenario in orange.

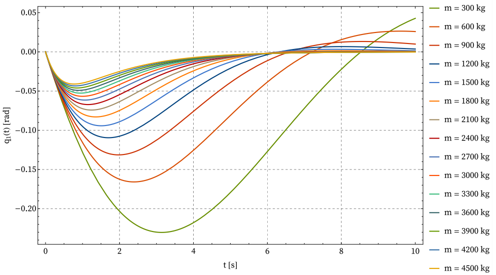

Figure 16: Parametric plot of the first joint's time evolution, first simulation. The real mass is 3000 kg.

- Derivative Roots:

$$
\begin{gathered}
\tilde{m}\ddot{q} + \hat{m}k_d\dot{q} + \hat{m}k_p(q - q_d) = 0 \\
\tilde{m}\ddot{q} + \hat{m}k_d\dot{q} + \hat{m}k_p q = \hat{m}k_p q_d \\
q(t) = q_d\left[1 - \frac{e^{-\xi\omega_n t}}{\sqrt{1-\xi^2}}\sin\left(\omega_d t + \theta\right)\right] + \left[q_0\cos\left(\omega_d\right)t + \frac{\dot{q}_0 + \xi\omega_n q_0}{\omega_d}\sin\left(\omega_d t\right)\right]e^{-\xi\omega_n t} \\
\tan\left(\sqrt{1-\xi^2}\,\omega_n t^*\right) = \beta(\xi)
\end{gathered}
\tag{38}
$$

- Damping coefficient and natural frequency fit: non-linear regression of closed-form solution, parameters are ξ and ω_n.

Coupled Solution

6.0 Mass and Velocity Retrieval:

- Continous Domain: solve coupled equations with Wolfram's `ParametricNDSolve` $\rightarrow q(m,t)$:

$$\Gamma(m) = \int_0^T \left[q(m,t) - q_{data}(t)\right]^2 \quad (39)$$
$$m^* = \min_m \Gamma(m)$$

- Discrete Domain: equations solved with Maple, closed-form solution:

$$\Gamma(m) = \sum_{k=0}^{N_p} \left[q(m, \frac{T}{N_p}k) - q_{data}(\frac{T}{N_p}k)\right]^2 \quad (40)$$

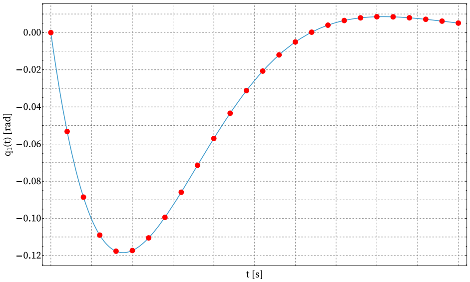

Figure 17: In blue is the continous solution, in red is the discretized one.

Velocity Extraction

- From final velocities relation:

$$\dot{p}_f = G^{-1} H \tag{41}$$

we can write:

$$\begin{aligned} H &= G\dot{p}_f \\ \Rightarrow M\dot{p}_i + J^T (J_O^+)^T M_O \dot{\psi}_i &= G\dot{p}_f \\ \Rightarrow \dot{\psi}_i &= M_O^{-1} J_O^T (J^+)^T (G\dot{p}_f - M\dot{p}_i) \end{aligned} \tag{42}$$

- Good results for translational velocities, big numerical erros for $\dot{\theta}_O$.
- Previous assumption: docking ($\dot{\theta}_O \approx 0$).

Table of Contents
7.0 Results:

Mass Extraction

7.0 Results:

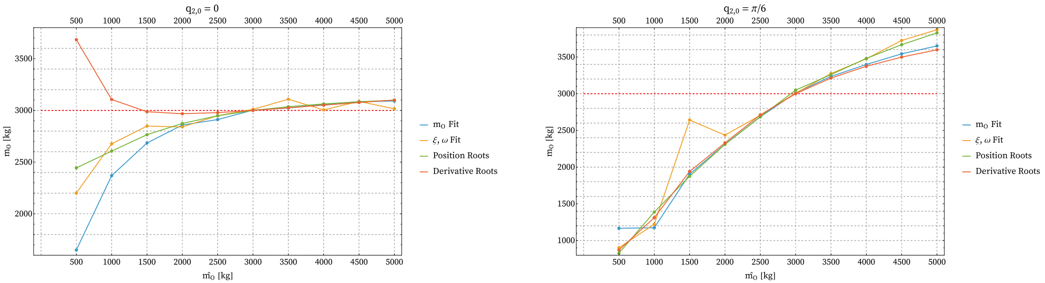

(a) (b)

Figure 18: Joints' Decoupling.

Mass Extraction

7.0 Results:

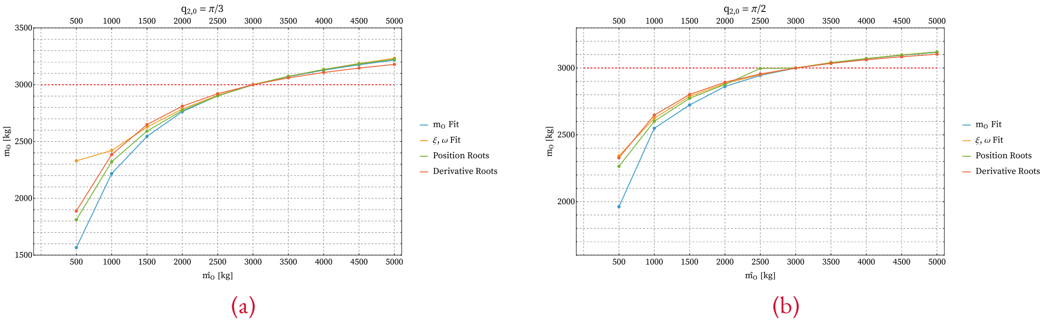

Figure 19: Joints' Decoupling.

Mass Extraction

7.0 Results:

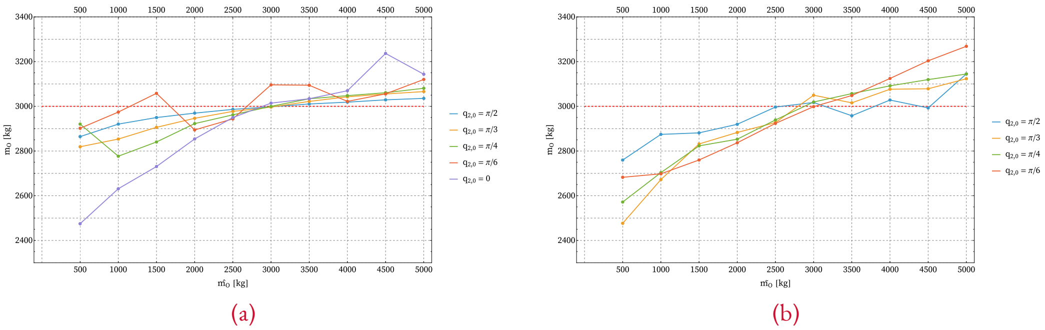

Figure 20: Coupled Solution.

Velocity Extraction

7.0 Results:

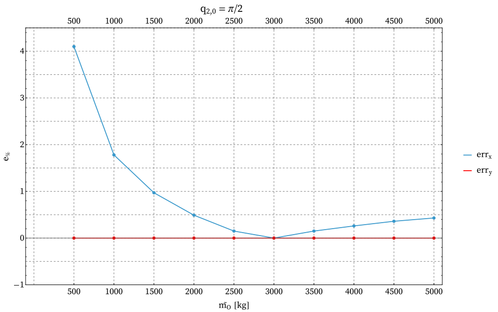

(a)

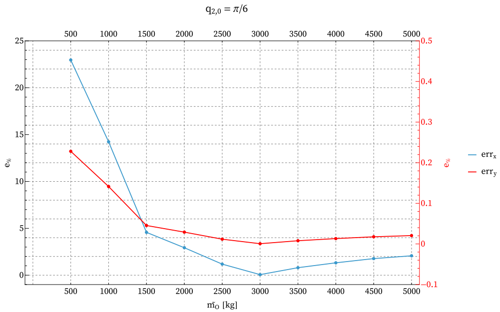

(b)

Figure 21: Velocity error for Simulation 1.

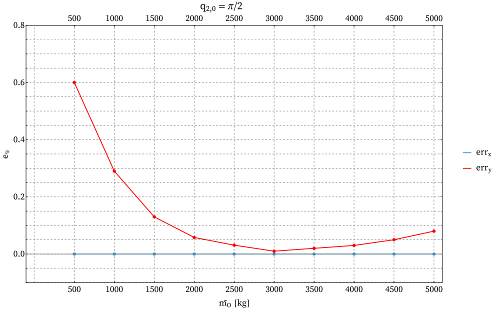

(a)

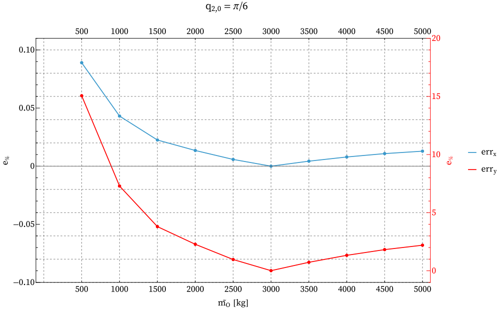

(b)

Figure 22: Velocity error for Simulation 2.

- Joints' Decoupling:
  - Pro: simple closed-form equation
  - Cons: depend significantly on VMS configuration.
  - ξ and ω_n fit best one.
  - When $\hat{m} > m$ better results: displacement is smaller, linerization error reduced.
- Coupled Solution:
  - Pro: less susceptible to VMS configuration.
  - Cons: require more computational power (continuous method).
  - Discrete method is faster ($\approx$ 0.03 s vs 1.5 s)

References

[1] ESA, "European robotic arm (era)," 1999. https://www.eoportal.org/satellite-missions/iss-era [Access: 11/03/2025)].

[2] "Mobile servicing system." https://it.wikipedia.org/wiki/Mobile_Servicing_System [Access: 11/03/2025)].

[3] ESA, "European robotic arm (era)," 1999. https://www.esa.int/esearch?q=era [Access: 04/03/2025)].

[4] G. Legnani, F. Casolo, P. Righettini, and B. Zappa, "A homogeneous matrix approach to 3d kinematics and dynamics—i. theory," *Mechanism and machine theory*, vol. 31, no. 5, pp. 573–587, 1996.

[5] G. Legnani, F. Casalo, P. Righettini, and B. Zappa, "A homogeneous matrix approach to 3d kinematics and dynamics—ii. applications to chains of rigid bodies and serial manipulators," *Mechanism and machine theory*, vol. 31, no. 5, pp. 589–605, 1996.

[6] C. Xavier, K. Sun-Wook, I. Michel, M. Arun, and J. Gilbert, "Post-impact dynamics of two multi-body systems attempting docking/berthing," *Acta Astronautica*, vol. 40, no. 11, pp. 759–769, 1997.

[7] R. J. Theodore and A. Ghosal, "Comparison of the assumed modes and finite element models for flexible multilink manipulators," *The International journal of robotics research*, vol. 14, no. 2, pp. 91–111, 1995.

Q & A

Thank you for listening!

Table of Contents

9.0 Q&A:

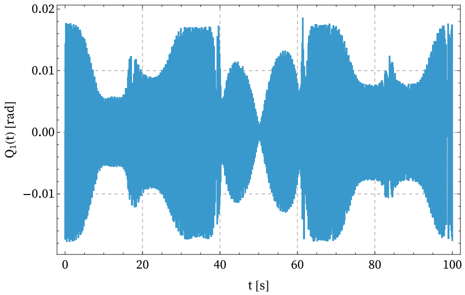

(a) *First joint.*

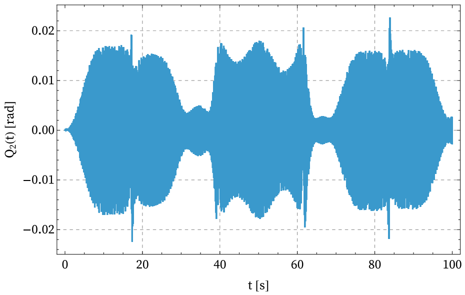

(b) *Second joint.*

Figure 23: Extended temporal window of joints' elastic coordinates for Simulation 1. The oscillations change in time due to the movement of the arms.

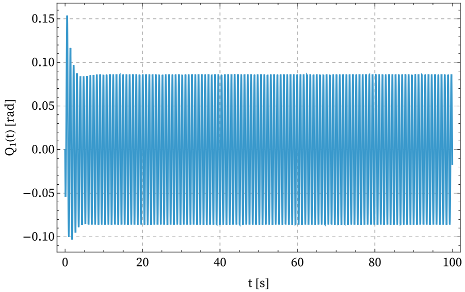

(a) *First joint.*

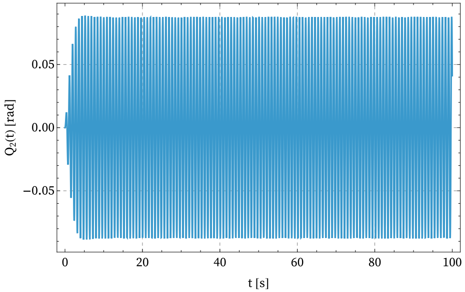

(b) *Second joint.*

Figure 24: Extended temporal window of joints' elastic coordinates for Simulation 1. The oscillations are constant since the arms do not move after the impact.

Elastic Bodies

9.0 Q&A:

- Elastic potential energy:

$$U = \frac{1}{2}\int_0^{l_i} ES\left(\frac{\partial^2 w(x,t)}{\partial x^2}\right)^2 dx$$
$$= \frac{1}{2}\int_0^{l_i} ES\left(\frac{\partial^2 W(x)}{\partial x^2} Q(t)\right)^2 dx \tag{43}$$

- Included in the stiffness matrix:

$$\frac{d}{dt}\frac{\partial U}{\partial \dot{Q}_i} - \frac{\partial U}{\partial Q_i} = 0 - Q(t)\int_0^{l_i} ES\frac{\partial^2 W(x)}{\partial x^2}\,dx$$
$$M\ddot{p} + C + Kp = u + J^T f_I \tag{44}$$
$$K_i = \int_0^{l_i} E_i S_i \frac{\partial^2 W_i(x)}{\partial x^2}\,dx$$